Purinergic Signalling (2016) 12:465–478
DOI 10.1007/s11302-016-9512-9

ORIGINAL ARTICLE

Coupling switch of P2Y-IP_3 receptors mediates differential Ca^{2+} signaling in human embryonic stem cells and derived cardiovascular progenitor cells

Jijun Huang[1,2] · Min Zhang[1] · Peng Zhang[1] · He Liang[1,3] · Kunfu Ouyang[4] · Huang-Tian Yang[1,2,3]

Received: 29 December 2015 / Accepted: 4 April 2016 / Published online: 20 April 2016

Abstract Purinergic signaling mediated by P2 receptors (P2Rs) plays important roles in embryonic and stem cell development. However, how it mediates Ca^{2+} signals in human embryonic stem cells (hESCs) and derived cardiovascular progenitor cells (CVPCs) remains unclear. Here, we aimed to determine the role of P2Rs in mediating Ca^{2+} mobilizations of these cells. hESCs were induced to differentiate into CVPCs by our recently established methods. Gene expression of P2Rs and inositol 1,4,5-trisphosphate receptors (IP_3Rs) was analyzed by quantitative/RT-PCR. IP_3R3 knockdown (KD) or IP_3R2 knockout (KO) hESCs were established by shRNA- or TALEN-mediated gene manipulations, respectively. Confocal imaging revealed that Ca^{2+} responses in CVPCs to ATP and UTP were more sensitive and stronger than those in hESCs. Consistently, the gene expression levels of most P2YRs except $P2Y_1$ were increased in CVPCs. Suramin or PPADS blocked ATP-induced Ca^{2+} transients in hESCs but only partially inhibited those in CVPCs. Moreover, the $P2Y_1$ receptor-specific antagonist MRS2279 abolished most ATP-induced Ca^{2+} signals in hESCs but not in CVPCs. $P2Y_1$ receptor-specific agonist MRS2365 induced Ca^{2+} transients only in hESCs but not in CVPCs. Furthermore, IP_3R2KO but not IP_3R3KD decreased the proportion of hESCs responding to MRS2365. In contrast, both IP_3R2 and IP_3R3 contributed to UTP-induced Ca^{2+} responses while ATP-induced Ca^{2+} responses were more dependent on IP_3R2 in the CVPCs. In conclusion, a predominant role of $P2Y_1$ receptors in hESCs and a transition of P2Y-IP_3R coupling in derived CVPCs are responsible for the differential Ca^{2+} mobilization between these cells.

Keywords P2Y receptors · IP_3 receptors · Ca^{2+} signaling · Pluripotent stem cells · Lineage progenitors

Jijun Huang and Min Zhang are joint first co-authors.

Electronic supplementary material The online version of this article (doi:10.1007/s11302-016-9512-9) contains supplementary material, which is available to authorized users.

✉ Huang-Tian Yang
htyang@sibs.ac.cn

[1] Key Laboratory of Stem Cell Biology, Institute of Health Sciences, Shanghai Institutes for Biological Sciences, Chinese Academy of Sciences and Shanghai Jiao Tong University School of Medicine, Shanghai 200031, China

[2] Second Affiliated Hospital, Zhejiang University, Hangzhou, Zhejiang 310009, China

[3] Translational Medical Center for Stem Cell Therapy, Shanghai East Hospital, Tongji University School of Medicine, Shanghai 200120, China

[4] Drug Discovery Center, Key Laboratory of Chemical Genomics, Peking University Shenzhen Graduate School, Shenzhen 518055, China

Introduction

Human embryonic stem cells (hESCs) are pluripotent cells with the properties of self-renewal and differentiation potential into various cell types, including cardiovascular progenitor cells (CVPCs [1–4]). This in vitro differentiation system provides unique tools for the study of early cardiovascular development [5], drug screening [6, 7], cytotoxicity testing [8, 9], and cardiac regenerative therapy [10, 11]. However, the physiological and pharmacological properties of hESCs and CVPCs, such as the Ca^{2+} signaling and the response to various modulators, are largely unknown. Such knowledge will promote the pharmacological regulation of lineage-specific commitment, the quality control of hESC derivatives from functional perspectives, and subsequently benefit the preclinical and clinical study of these cells.

Nucleotides, such as ATP, have been shown to play a fundamental role in the cardiovascular system under physiological and pathological conditions through the activation of specific purinergic receptors [12–14]. Extracellular nucleotide-activated membrane P2 receptors (P2Rs) are composed of seven mammalian P2X receptors (P2XRs) acting as Ca^{2+} channels and eight mammalian P2Y receptors (P2YRs) coupling to G proteins [15]. Both P2XRs and P2YRs are widely expressed in early developing embryos, suggesting that they may play roles in various cell types [16]. However, little is known about the difference of P2R subtype-mediated Ca^{2+} signals between the hESCs and CVPCs, a gap for the application of these cells in drug development and cytotoxicity testing.

P2R activation-mediated Ca^{2+} signals have been shown to regulate the physiological responses in the cardiovascular system, such as endothelial cells [17, 18], smooth muscle cells [19, 20], and cardiomyocytes [21, 22]. They are also involved in the proliferation and cardiac differentiation of mouse (m) ESCs [23, 24] and the growth of human adult cardiac progenitors [25]. In addition, G protein-mediated Ca^{2+} signals play a role in the maintenance of undifferentiated state of hESCs [26]. ATP has been verified to induce Ca^{2+} transients in hESCs and derived cardiomyocytes [27]. However, the contribution of P2Rs to extracellular nucleotide-mediated Ca^{2+} signals in the hESCs and the derived CVPCs is largely unknown.

The activation of $G_{q/11}$-protein coupled P2YR subtypes elicits intracellular Ca^{2+} release via inositol 1,4,5-trisphosphate receptors (IP_3Rs) on the endoplasmic reticulum [28]. IP_3Rs consist of three subtypes, termed IP_3R1, IP_3R2, and IP_3R3, and have a tissue-specific distribution relating to their physiological and pharmacological responses in various tissues [29, 30], including cardiovascular systems [31–33]. However, the roles and the functional coupling of P2Rs and IP_3R subtypes in hESCs and derived CVPCs remain unclear.

Thus, the aims of this study are to determine (i) the expression pattern of P2Rs and IP_3Rs in hESCs and derived CVPCs; (ii) the Ca^{2+} responses of these cells to multiple extracellular nucleotides (ATP, UTP, ADP, and UDP) and P2R-targeted reagents; and (iii) the contribution of IP_3R subtypes to P2R-mediated Ca^{2+} signals.

Methods

hESC culture and CVPC induction

hESC culture and CVPC induction were carried out as described previously [4, 34]. Briefly, hESC lines H7 and H9 (WiCell Research Institute, Madison, WI, USA) were routinely maintained in mTeSR1 media (Stem Cell Technologies, Vancouver, Canada) on Matrigel- (hESC qualified; Corning, New York, NY, USA) coated dishes. For CVPC induction, hESCs with density of 80 % confluence were digested into single cells by Accutase (Stem Cell Technologies, Vancouver, Canada) and seeded onto Matrigel-coated dishes at a density of 3.5×10^4 cells cm^{-2} in CVPC induction medium (CIM) for 3 days. CIM contained DMEM/F12, 1 × B27 supplement without vitamin A, 1 % L-glutamine, 1 % penicillin/streptomycin (Life Technologies, Carlsbad, CA, USA), and supplemented with 400 μM 1-thioglycerol (Sigma, Saint Louis, MO, USA), 50 μg mL^{-1} ascorbic acid (Sigma, Santa Clara, CA, USA), 25 ng mL^{-1} bone morphogenetic protein 4 (R&D Systems, Minneapolis, MN, USA), and 3 μM Glycogen synthase kinase 3 (GSK3) inhibitor CHIR99021 (Axon Medchem, Groningen, Netherlands).

For Ca^{2+} imaging, hESCs were digested into single cells by Accutase and seeded onto Matrigel-coated 20 mm glass-bottom dishes (Nest Scientific, Rahway, NJ, USA) at a density of 3.5×10^4 cells cm^{-2} in mTeSR1 or CIM. The medium was changed every day. Of 36–48 h after seeding, hESC clones were used for Ca^{2+} imaging to allow homogenous loading of the Ca^{2+} indicator. CVPCs on day 3 of differentiation were used for Ca^{2+} imaging. To reduce apoptosis, 5 mM Rock inhibitor Y27632 (Stem Cell Technologies, Vancouver, Canada) was added for the first 24 h after cell seeding. The embryoid body (EB) differentiation assay was performed according to the previous report [35].

Immunostaining

Immunostaining assays were performed as previously described [34]. Briefly, cells were fixed with 4 % paraformaldehyde and permeabilized in 0.3 % Triton X-100 for intracellular antigens (Sigma, Saint Louis, MO, USA), blocked in 10 % normal goat serum (Vector Laboratories, Burlingame, CA, USA) and then incubated with primary antibodies against MESP1 (1:100; Aviva Systems Biology, San Diego, CA, USA), MEF2C (1:100; Cell Signaling Technology, Danvers, MA, USA), ISL1 (1:100; Developmental Studies Hybridoma Bank, Iowa City, IA, USA), Oct4 (1:200; Abcam, Cambridge, UK), or SSEA4 (1:100; Millipore, Temecula, CA, USA) at 4 °C overnight and detected by DyLight 488- or 549-conjugated secondary antibodies (Jackson ImmunoResearch Laboratories, West Grove, PA, USA). Nuclei were stained with DAPI (Sigma, Saint Louis, MO, USA). A Zeiss Observer microscope was used for slide observation and image capture.

Flow cytometry analysis

Cells were harvested and dissociated by Accutase (Stem Cell Technologies, Vancouver, Canada). Samples were blocked by 3 % fetal bovine serum and then stained for the presence of appropriate hESCs or CVPCs markers using antibodies including PE-conjugated SSEA1 (1:20; eBioscience, San

Diego, CA, USA), PE-conjugated SSEA4 (1:100; BD Biosciences, San Jose, CA, USA), and un-conjugated SOX2 (1:100; R&D Systems, Minneapolis, MN, USA) with PE-conjugated secondary antibody (1:200; eBioscience, San Diego, CA, USA) or isotype-matched negative controls.

Ca^{2+} imaging

hESCs or CVPCs were loaded with 2.5 μM Fluo4-AM (Life Technologies, South San Francisco, CA, USA) dissolved in the extracellular bath solution for 30 min at 37 °C [27]. Then the Ca^{2+} indicator was washed out for three times by the bath solution and the cells were used 30 min later at room temperature for the de-esterification of the dye. The fluorescence of hESCs or CVPCs was measured using a confocal laser scanning microscope (LSM 710, Carl Zeiss, Oberkochen, Germany) with a ×20 objective. The fluorescence intensity was excited with wavelength 488 nm and the emission was collected with wavelength >493 nm. Images were acquired every 2 s.

Analysis of Ca^{2+} responses

The analysis of Ca^{2+} responses was based on the customer-modified Interactive Data Language (IDL, ITT corporation, White Plains, NY, USA) Program, Flash Sniper reported previously [36]. Briefly, the images recorded were opened by Flash Sniper and a mask was set up to exclude the noise signals from non-cell regions. The region of interest (ROI) was manually selected for each cell. The normalized amplitude of a Ca^{2+} transient was expressed as $dF/F_0 = (F_1 - F_0)/F_0$, where F_0 and F_1 are the values of the fluorescence at rest and the peak time point, respectively. For each ROI, the start-time and end-time of Ca^{2+} transients were set manually and dF/F_0 was calculated by Flash Sniper. Finally, the traces representing the fluorescence changes were automatically generated by the software. The cell with $dF/F_0 > 0.2$ was defined as a responding cell. For the calculation of amplitude values, the counted cell number of randomly selected responding cells in each field is commonly >50, while all the responding cells were chosen when the total responding cell number is <50 in the experiment with some reagents. All the cells in each field of imaging were counted for calculating the responding percentage. The responding cell percentage was calculated as responding cell number/total cell number examined. At least three independent experiments were done for each concentration of the reagents.

Reverse transcription (RT)-PCR and quantitative real-time PCR (Q-PCR)

Total RNA was prepared using an RNeasy Plus Mini Kit (QIAGEN, Hilden, Germany) following the manufacturer's instructions and treated with RNase-Free DNAse (Promega, Madison, WI, USA) for 15 min to eliminate the potential contamination of genomic DNA. cDNAs were generated by reverse-transcribed total RNA (1 μg) using ReverTra Ace reverse transcriptase (Toyobo, Osaka, Japan). The RT-PCR was carried out using 2× Taq Plus Master Mix (Vazyme, Piscataway, NJ, USA). *GAPDH* was used as endogenous control, and samples without reverse transcription were used as negative controls. Q-PCR was performed and analyzed by the ViiA™ 7 Real-Time PCR System (Life Technologies, Carlsbad, CA, USA) with SYBR Green Q-PCR Master Mix (Toyobo, Osaka, Japan). Q-PCR data were expressed as fold changes normalized to internal control *GAPDH*. The RT-PCR and Q-PCR primers were selected from the Primer Bank and were listed in Supporting Information Table S1.

Knockout (KO) and knockdown (KD) of IP_3Rs

IP_3R2KO cell lines were established by electroporation using the hESC Nucleofector® Kit (Lonza, Basel, Switzerland) with the transcription activator-like effector nucleases (TALEN) plasmids (Viewsolid Biotech, Beijing, China) targeting 5′-CCA GCT TCC TCT ACA T-3′ (the left target) and 5′-ACG CGG AGG GCT CGG TC-3′ (the right target) of the first exon of *ITPR2* (the gene of IP_3R2, Online Resource Fig. S1a). Single clones were selected by puromycin and two clones of IP_3R2KO (IP_3R2KO-6 and IP_3R2KO-12) from H7 hESCs were confirmed by sequencing and Western blot. To establish IP_3R3KD hESCs, short hairpin (sh) RNA-mediated mRNA interference were used and the two 19-bp sequences (5′-GAA GTT CCG TGA CTG CCT C-3′ and 5′-GAG GCA GTC ACG GAA CTT C-3′ [37]) were cloned into the pLKO1 vector containing puromycin-resistant gene (Online Resource Fig. S1b). The vector control was pLKO1 vector inserted with non-targeted sh-RNA sequence (Sigma, Saint Louis, MO, USA). The H9 and H7 hESCs were transfected by the lentivirus constructed with the above vectors and selected by puromycin (Life Technologies, Carlsbad, CA, USA) at 1 mg mL^{-1}. Single clones were picked out and amplified. Two clones of IP_3R3KD from either H9 ($siIP_3R3$-1 and $siIP_3R3$-2) or H7 ($siIP_3R3$-a and $siIP_3R3$-b) hESCs were used in this study.

Western blot analysis

Total membrane fractions of hESCs and CVPCs were prepared as previously reported [24] and were separated on 8 % SDS-PAGE gels and transferred to Nitrocellulose Blotting Membranes. The antibodies against IP_3R1 and IP_3R2 were made as previously reported [38]. The antibodies against IP_3R1 (1:1000), IP_3R2 (1:1000), IP_3R3 (1:1000; BD Biosciences, San Jose, CA, USA), and β-actin (1:8000; Sigma, Saint Louis, MO, USA) were used. Then the membranes were incubated with IRDye 680LT Donkey anti-Rabbit IgG or IRDye 800LT Donkey anti-mouse IgG (1:8000; Li-

COR Biosciences, Lincoln, NE, USA) as secondary antibodies and visualized on an Odyssey Infrared Imager (Li-COR Biosciences, Lincoln, NE, USA).

Reagents and solutions

(*N*)-Methanocarba-2-MeSADP (MRS2365), 2-methylthio-ATP (2-MeSATP), and 2-chloro-N^6-methyl-(*N*)-methanocarba-2′-deoxyadenosione-3′,5′-bisphosphate (MRS2279) were purchased from Tocris Biosciences Ltd (Bristol, UK). All the other reagents, including ATP, UTP, ADP, UDP, 2′(3′)-*O*-(4-Benzoylbenzoyl)-ATP (BzATP), pyridoxal phosphate-6-azophenyl-2′,4′-disulfonic acid (PPADS), suramin, and 2-aminoethoxydiphenyl borate (2-APB) were purchased from Sigma (Saint Louis, MO, USA). Reagents were all directly dissolved in distilled water except PPADS and 2-APB which were dissolved in DMSO. The extracellular bath solution contains (in mM) NaCl, 135; KCl, 5.4; $CaCl_2$ 1.8; $MgCl_2$ 1.0; glucose, 10; and HEPES, 10 (pH adjusted to 7.4). For Ca^{2+}-free solution, extracellular $CaCl_2$ was removed and 1 mM EGTA was added.

Statistical analysis

The data were presented as means ± SEM. Two-tail *t* test was used to analyze the data obtained from Q-PCR assays; one-way ANOVA with Dunnett's multiple comparison tests were used to analyze the responding cell percentage of hESCs or CVPCs pre-treated with Ca^{2+}-free solution, suramin, PPADS, or 2-APB vs. ATP alone, and to analyze the responding cell percentage to MRS2365 in hESCs vs. CVPCs. Two-way ANOVA with Bonferroni post-test was used to analyze the responses to ATP or 2MeSATP in hESCs with or without MRS2279. Two-way ANOVA with Dunnett's multiple comparison tests were used to analyze the data of responding cell percentage to ADP in hESCs vs. that in CVPCs and to MRS2365 in IP_3R2KO hESCs vs. wild type (WT) cells; the Hill slopes and EC_{50} values of the concentration-response curves were calculated using nonlinear regression (variable slope), and the slopes of concentration-amplitude curves were calculated using linear regression. All the statistical analyses were performed by GraphPad Prism5 (San Diego, CA, USA). $P < 0.05$ was considered statistically significant.

Results

Differential Ca^{2+} responses to the P2R stimulation in hESCs and derived CVPCs

H9 and H7 hESCs had typical morphology and pluripotent characteristics, such as alkaline phosphatase activity (ALP, Fig. 1a) and the expression of pluripotent markers SSEA4 and SOX2 (Fig. 1b), while the derived CVPCs expressed ISL1/MESP1/MEF2C/SSEA1 (Fig. 1c) as previously reported [4, 34].

To determine the function of P2Rs in hESCs and derived CVPCs, we measured intracellular Ca^{2+} responses to various nucleotides in these cells. hESCs and CVPCs showed different responding patterns of intracellular Ca^{2+} activities to extracellular nucleotides in a concentration-dependent manner. UTP, a $P2Y_{2,4}$ receptor agonist [39], up to 300 μM only induced Ca^{2+} signals in 34.6 ± 6.3 % (H9) and 18.4 % ± 3.4 % (H7) of hESCs but in almost all CVPCs (Fig. 2a, b), while the non-specific P2R agonist ATP (100 μM) triggered intracellular Ca^{2+} responses in almost all hESCs and CVPCs (Fig. 2a, c).

The concentration-response curves for UTP (Fig. 2b) and ATP (Fig. 2c) significantly shifted to left in the CVPCs compared with those in the hESCs, indicating that the CVPCs are more sensitive to UTP and ATP than hESCs. The EC_{50} values of UTP were more than 40-fold higher in hESCs than those in CVPCs (Fig. 2b). The EC_{50} values of ATP were more than ninefold higher in hESCs than those in CVPCs (Fig. 2c). Moreover, the amplitude of Ca^{2+} transients induced by UTP or ATP was concentration-dependently increased in both hESCs and CVPCs, but the amplitude was significantly higher in the CVPCs than in the hESCs (Fig. 2d, e). Further, the slopes of concentration-amplitude curves to UTP in CVPCs were nearly twofold higher than those in hESCs (Fig. 2d), while those to ATP were slightly higher in CVPCs than in hESCs (Fig. 2e).

ADP, a $P2Y_{1,12,13}$ receptor agonist [39], at 100 or 500 μM induced the Ca^{2+} responses in most hESCs and CVPCs (Fig. 3a). However, hESCs showed higher Ca^{2+} responding percentage than that of CVPCs at lower concentration of ADP (10 μM, Fig. 3b). There is no Ca^{2+} response to UDP (up to 500 μM), a $P2Y_6$ receptor agonist [39], in hESCs (Fig. 3c, d), while CVPCs were concentration-dependently activated by UDP (Fig. 3d).

These results demonstrate that the hESCs, at least H7 and H9 cell lines, and their derived CVPCs respond different Ca^{2+} activities to extracellular nucleotides. Especially, CVPCs have significantly higher sensitivity and amplitude of Ca^{2+} transients responding to UTP and ATP comparing with the hESCs.

Gene expression patterns of P2Rs and IP_3Rs in hESCs and CVPCs

To determine whether the different nucleotide-induced Ca^{2+} activities between hESCs and CVPCs are related to the transition of P2Rs, we analyzed their gene expression patterns. RNA samples from day 18 EBs differentiated from hESCs were used as positive controls. The expression of *P2RX2*, *P2RX5*, *P2RX7*, *P2RY1*, *P2RY2*, *P2RY6*, and *P2RY12* was detected in both H9 and H7 hESCs (Fig. 4a). The expression patterns of P2Rs were different in the CVPCs. *P2RX1*, *P2RX2*, and *P2RX6* were hardly detected, while *P2RX3* and

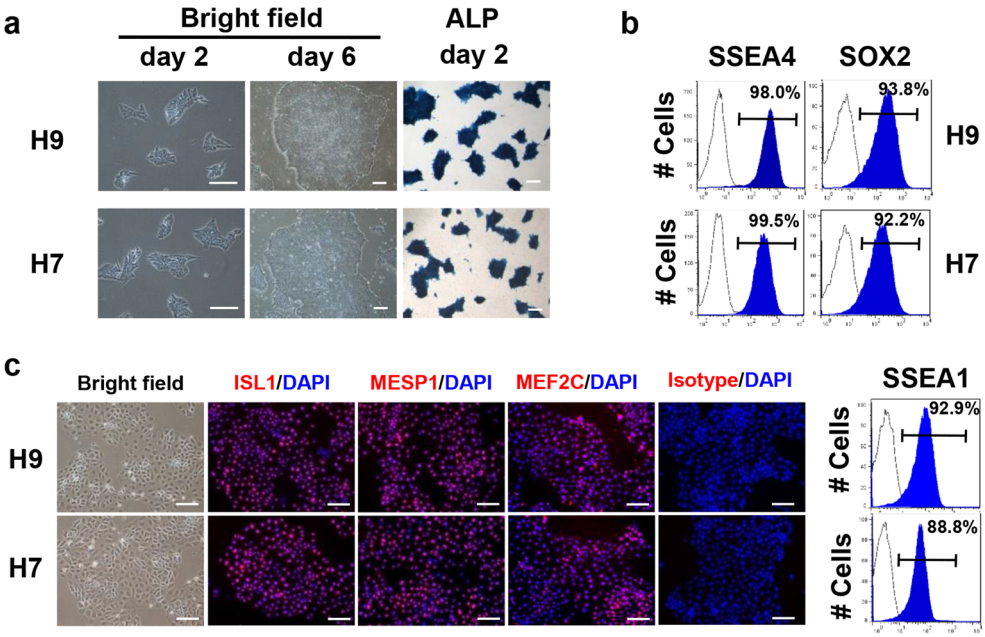

Fig. 1 The maintenance of hESCs and directed differentiation to CVPCs. **a** Morphology and alkaline phosphatase (ALP) activity of H9 and H7 hESCs on day 2 and day 6 after passage. *Scale bar*, 100 μm. **b** Flow cytometry analysis of the $SSEA4^+$ and $SOX2^+$ cell percentage in H9 and H7 hESCs. **c** Immunostaining of CVPC markers ISL1, MESP1, or MEF2C (*red*) with a nucleus marker DAPI (*blue*) and flow cytometry analysis of the $SSEA1^+$ H9 and H7 CVPCs. *Scale bar*, 50 μm

P2RX4 were increased but *P2RX5* and *P2RX7* were decreased in the CVPCs compared with the hESCs (Fig. 4a). Q-PCR analysis further confirmed the significantly lower expression levels of *P2RX2*, *P2RX5*, and *P2RX7* and higher expression levels of *P2RX3* and *P2RX4* in the CVPCs than in the hESCs (Fig. 4b). The expression of most *P2RY* genes were 7-fold to 60-fold higher in the CVPCs than those in the hESCs, including those hardly detected in the hESCs, such as the genes encoding $P2Y_{4,11,14}$ receptors (Fig. 4a, b). In contrast, only the expression of *P2RY1* was reduced by 75 % in the CVPCs compared with that in the hESCs (Fig. 4b). These data indicate the transition of P2R gene expression patterns between the hESCs and CVPCs.

Because some P2YRs elicit Ca^{2+} release from intracellular Ca^{2+} store via activating IP_3Rs [39], we then compared the expression of three genes encoding for IP_3R subtypes [29, 40]. It is noteworthy that the expression levels of all three *ITPR*s encoding IP_3Rs were significantly lower in CVPCs than in hESCs (Fig. 4a, c), which was contradictory to the observed stronger Ca^{2+} response in the CVPCs. These results suggest that the gene expression patterns of P2Rs and IP_3Rs may account for the different intracellular Ca^{2+} responses to the above nucleotides in the two cell types examined.

Differential P2YR subtypes linking to IP_3Rs account for distinct Ca^{2+} responses in hESCs and CVPCs

To further clarify the contribution of P2Rs to the different kinetics of nucleotide-stimulated Ca^{2+} mobilization in hESCs and CVPCs, we pre-incubated the cells with extracellular Ca^{2+}-free solution to block the Ca^{2+} entry through membrane P2XRs [41] as shown in Fig. 5a. The extracellular Ca^{2+}-free condition did not significantly alter the percentage of cells responding to ATP and only slightly decreased the amplitude of Ca^{2+} transients in H9 hESCs and derived CVPCs (Fig. 5b–d), indicating that little effects of P2XRs are involved. Then suramin, a nonselective antagonist of P2Rs except $P2Y_4$ receptor, and PPADS, a nonselective antagonist of most P2XRs and $P2Y_{1,4,6,13}$ receptors [42], were applied to detect the involvement of P2YRs (Fig. 5a). Pretreatment of 100 μM suramin or 50 μM PPADS reversibly blocked almost all the Ca^{2+} events induced by ATP in hESCs (Fig. 5b–d). In contrast, they only partially inhibited the proportion of Ca^{2+} responding cells (Fig. 5c) and the amplitude of Ca^{2+} transients (Fig. 5d) in the CVPCs, even up to 200 μM suramin or 100 μM PPADS (data not shown). Similar results were observed in H7 hESCs and CVPCs (Online Resource Fig. S2). These results suggest that distinct P2YR subtypes regulate Ca^{2+} signals in hESCs and derived CVPCs, while the contribution of P2XRs is trivial.

Since IP_3Rs were the critical downstream mediators of the $G_{q/11}$-coupled $P2Y_{1,2,4,6,11}$ receptors [39], we then examined whether IP_3Rs were involved in the ATP-induced Ca^{2+} activities. The IP_3R inhibitor 2-APB at 100 μM [43] did not affect the baseline of Ca^{2+} signals in H9 hESCs and CVPCs (Fig. 5b), while it completely and reversibly inhibited the percentage of ATP-activated Ca^{2+} events in the hESCs and largely attenuated the proportion of Ca^{2+} responding CVPCs by about 90 % (Fig. 5c) accompanied with a significant decrease of the amplitudes of Ca^{2+} transients (Fig. 5d). Similar results were observed in H7 hESCs and derived CVPCs (Online Resource Fig. S2). These results suggest an important role of IP_3Rs in the generation of P2YR-mediated Ca^{2+} signals following the ATP stimulation in both hESCs and CVPCs.

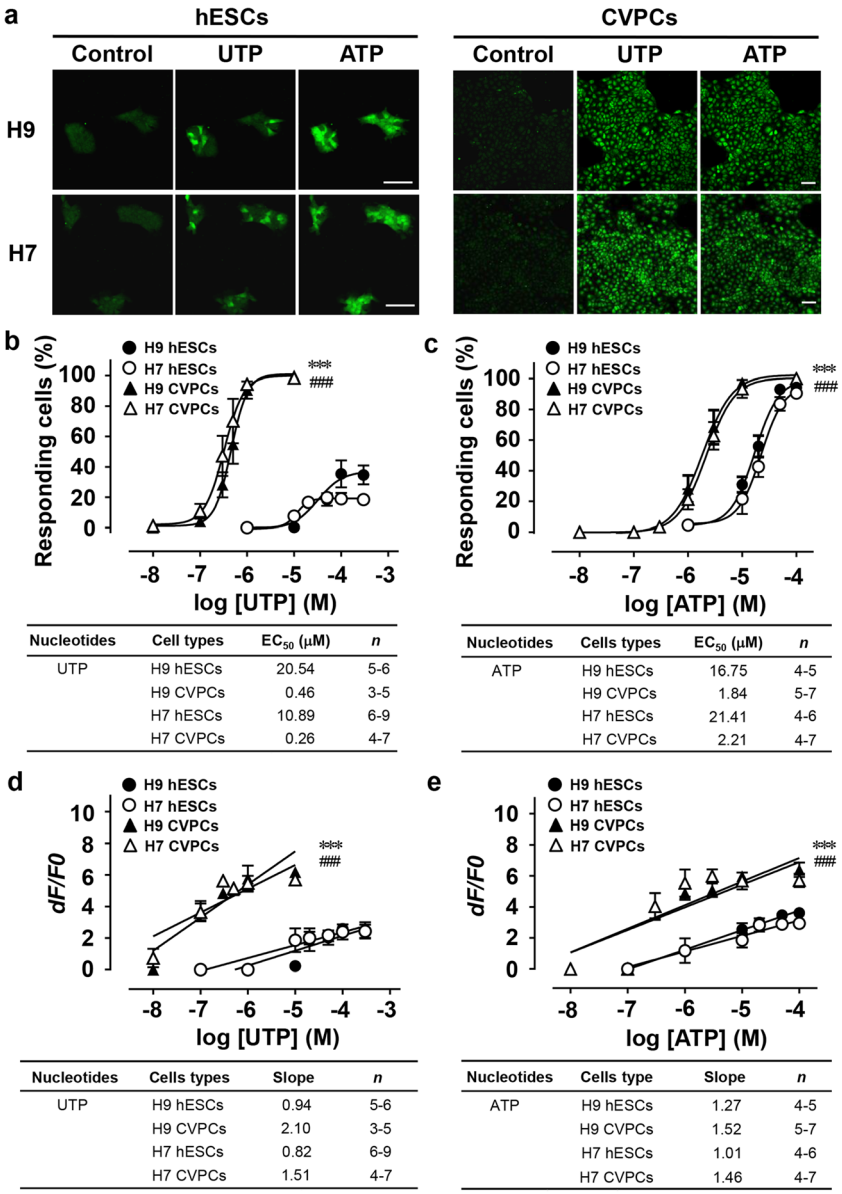

Nucleotides	Cell types	EC_{50} (μM)	n
UTP	H9 hESCs	20.54	5-6
	H9 CVPCs	0.46	3-5
	H7 hESCs	10.89	6-9
	H7 CVPCs	0.26	4-7

Nucleotides	Cells types	EC_{50} (μM)	n
ATP	H9 hESCs	16.75	4-5
	H9 CVPCs	1.84	5-7
	H7 hESCs	21.41	4-6
	H7 CVPCs	2.21	4-7

Nucleotides	Cells types	Slope	n
UTP	H9 hESCs	0.94	5-6
	H9 CVPCs	2.10	3-5
	H7 hESCs	0.82	6-9
	H7 CVPCs	1.51	4-7

Nucleotides	Cells type	Slope	n
ATP	H9 hESCs	1.27	4-5
	H9 CVPCs	1.52	5-7
	H7 hESCs	1.01	4-6
	H7 CVPCs	1.46	4-7

Fig. 2 Characteristics of Ca^{2+} signals induced by UTP and ATP in hESCs and derived CVPCs. **a** Representative confocal images showing the Ca^{2+} responses to UTP and ATP (both 100 μM) in hESCs (*left panel*) and derived CVPCs (*right panel*). *Scale bar*, 50 μm. **b**, **c** The concentration-response curves of UTP (**b**) and ATP (**c**) in hESCs and CVPCs. **d**, **e** The concentration-amplitude curves of Ca^{2+} transients to UTP (**d**) or ATP (**e**) in hESCs and CVPCs. $n = 5–9$ independent experiments for each concentration; 50–150 hESCs and 200–400 CVPCs in each experiment. $^{***}P < 0.001$ (H9) and $^{\#\#\#}P < 0.001$ (H7) CVPCs vs. corresponding hESCs

$P2Y_1$ receptors are predominant in hESCs but not in CVPCs

Based on the above observations, we hypothesized that $P2Y_1$ receptors would be critically responsible for the intracellular Ca^{2+} response in hESCs but not in CVPCs. To test it, we used a $P2Y_1$ receptor selective agonist (MRS2365), a P2X and $P2Y_1$ receptor nonselective agonist (2-MeSATP [44, 45]), and a $P2Y_1$ receptor selective antagonist (MRS2279 [46]). Firstly, the ATP-induced Ca^{2+} transients in hESCs were blocked by pre-incubation of 20 μM MRS2279 (Fig. 6a, b) but were not affected in CVPCs (Fig. 6c, d). MRS2279 pre-incubation decreased the percentage of responding cells to ATP by 91 % in H9 and 82 % in H7 hESCs compared with ATP alone but it was ineffective in CVPCs (Fig. 6e). Secondly, 2-MeSATP (50 μM) induced Ca^{2+} transients in more than 90 % hESCs, and these responses were almost completely blocked by MRS2279 (20 μM) (Fig. 6a, b, f). These data further confirmed that the function of P2XRs is trivial in hESCs. In contrast, only few CVPCs responded to 2-MeSATP (100 μM) stimulation (Fig. 6g). Thirdly, MRS2365 (50 μM), a $P2Y_1$ receptor selective agonist, induced Ca^{2+} transients in almost all hESCs (Fig. 6a, b, h), while no responses to MRS2365 were detected in the CVPCs up to 100 μM (Fig. 6c, d, h). Thus, $P2Y_1$ receptors appear to be a dominant P2R subtype in hESCs but not in CVPCs.

$P2Y_1$ receptor-mediated Ca^{2+} activities through IP_3R2 in hESCs

To identify the downstream IP_3Rs in the $P2Y_1$ receptor-activated Ca^{2+} signals in hESCs, we used downregulation

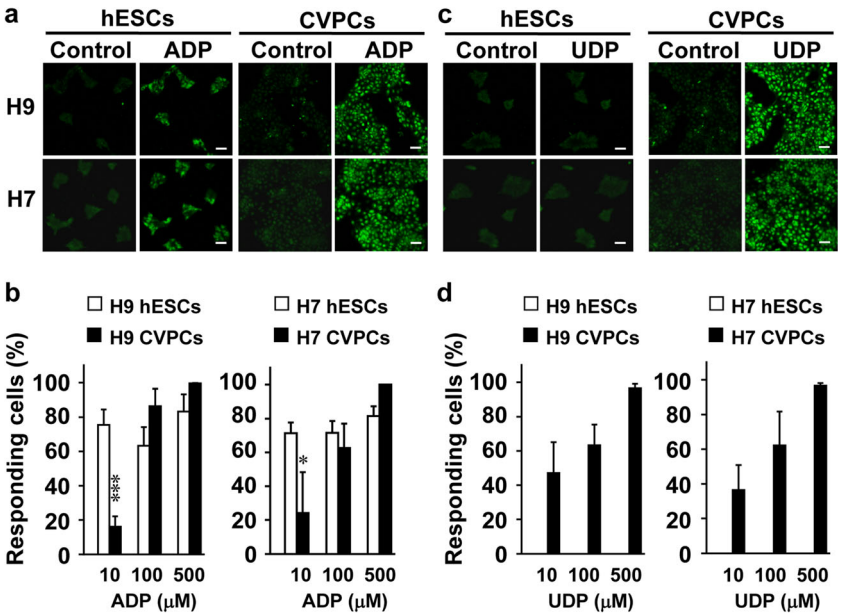

Fig. 3 Characteristics of Ca^{2+} signals induced by ADP and UDP in hESCs and derived CVPCs. **a** Representative confocal images of the Ca^{2+} responses to ADP (100 μM for hESCs, 500 μM for CVPCs). **b** The cell percentages with Ca^{2+} responses to ADP stimulation (10–500 μM) in hESCs and CVPCs. **c** Representative confocal images of the Ca^{2+} responses to UDP (500 μM) in hESCs and CVPCs. **d** The cell percentages with Ca^{2+} responses to UDP stimulation (10–500 μM) in hESCs and CVPCs. $n = 5$ independent experiments; 50–150 hESCs and 200–400 CVPCs in each experiment; $^{*}P < 0.05$, $^{***}P < 0.001$ vs. hESCs at the corresponding concentrations. *Scale bar*, 50 μm

and loss of function strategies. Since IP_3R1 was hardly detected at protein level in hESCs (Fig. 7a), we then examined the involvement of other two subtypes by establishment of IP_3R2KO and stable IP_3R3KD hESCs (Online Resource Fig. S1a, b). TALEN-mediated IP_3R2KO and shRNA-mediated IP_3R3KD ($siIP_3R3$) were confirmed by Western blot analysis (Fig. 7a, b). These cells showed pluripotent markers and ALP activity similar to the vector control and WT hESCs (Online Resource Fig. S1c). The $P2Y_1$ receptor-specific agonist MRS2365 concentration-dependently triggered Ca^{2+} responses in WT and vector control hESCs (Fig. 7c, d). These responses were not significantly altered in IP_3R3KD hESCs (Fig. 7c, d) but were rightward and downward shifted in IP_3R2KO cell lines (Fig. 7d). These data reveal that IP_3R2 plays an important role in $P2Y_1$ receptor-mediated Ca^{2+} activities in hESCs.

Differential coupling of IP_3R3 and IP_3R2 to ATP- and UTP-targeted P2YRs in CVPCs

Due to the negligible function of $P2Y_1$ receptor in CVPCs, the coupling of IP_3R2 and IP_3R3 to other P2YR-mediated Ca^{2+} signals in the CVPCs was examined. Our results showed that IP_3R3KD or IP_3R2KO hESC-derived CVPCs had comparable expression of CVPC marker SSEA1 between vector control and WT CVPCs (Online Resource Fig. S1d, e). IP_3R3KD did not alter the concentration-response curves of ATP in CVPCs (Fig. 7e, f), but right-shifted the curves of UTP (Fig. 7g, h), with the EC_{50} values 7-fold to 9.5-fold ($siIP_3R3$-1/2) and 3.5-fold to 7-fold ($siIP_3R3$-a/b) higher than those of vector control CVPCs (Table 1). However, IP_3R2KO right-shifted the concentration-response curves of both ATP (Fig. 7i) and UTP (Fig. 7j). The EC_{50} values of ATP were 17-fold (IP_3R2KO-6) and 12-fold (IP_3R2KO-12) higher than those of WT CVPCs, and the values of UTP were 38-fold (IP_3R2KO-6) and 17-fold (IP_3R2KO-12) higher than those of WT CVPCs (Table 1). In addition, the slopes of the curves were decreased in the IP_3R2KO CVPCs (Table 1). Furthermore, the averaged amplitudes of Ca^{2+} transients induced by ATP (300 nM to 10 μM) and UTP (100 nM to 3 μM) were decreased in IP_3R2KO CVPCs compared with those in WT CVPCs (Online Resource Fig. S3). These results suggest that both IP_3R2 and IP_3R3 contribute to the UTP/$P2Y_{2,4}$-mediated Ca^{2+} activities in the CVPCs, while ATP/P2YR-mediated Ca^{2+} signals are more dependent on the IP_3R2 in these cells.

Discussion

The main findings of the present study are that (i) extracellular nucleotides elicit distinct intracellular Ca^{2+} responses between hESCs and derived CVPCs, with more sensitive and stronger Ca^{2+} responses to ATP and UTP in CVPCs than those in hESCs; (ii) the expression of most genes encoding P2YRs except $P2Y_1$ receptors are higher in the CVPCs than those in the hESCs; (iii) $P2Y_1$ receptors primarily mediate nucleotide-induced Ca^{2+} activities in hESCs but not in CVPCs; and (iv) the different functional coupling between the P2YR subtypes and IP_3R subtypes contributes to the distinct intracellular Ca^{2+} signals in hESCs and CVPCs. These findings provide new insights into the physiological and pharmacological properties of hESCs and derived CVPCs by revealing critical roles of P2YRs and contributions of IP_3R subtypes in the regulation of Ca^{2+} signals via purinergic signaling pathways.

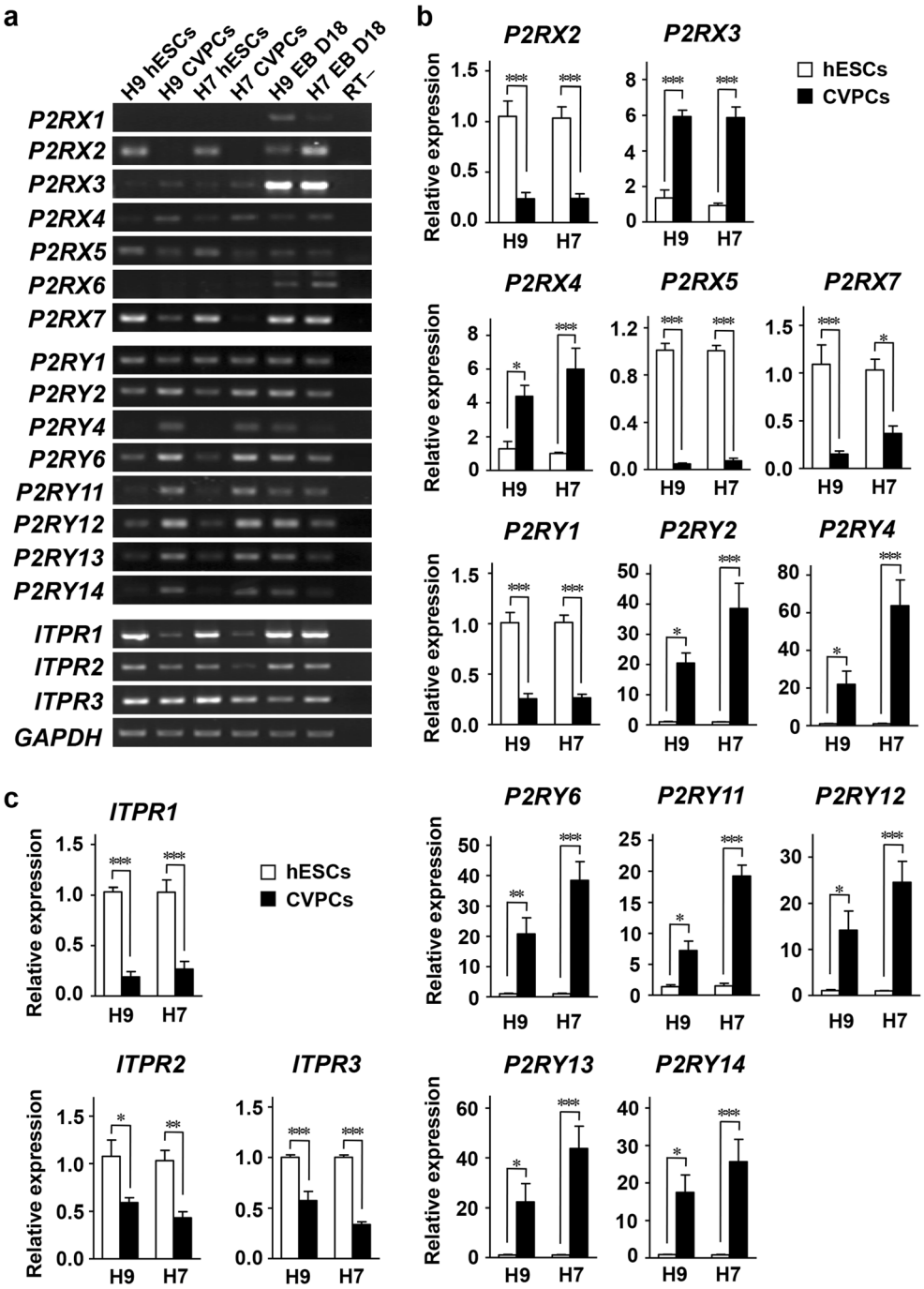

Fig. 4 Expression patterns of genes encoding P2Rs and IP_3Rs in hESCs and CVPCs. **a** RT-PCR analysis of gene expression of all mammalian subtypes of P2Rs and IP_3Rs in hESCs and CVPCs. EB, embryoid body. **b**, **c** Q-PCR analysis of the gene expression of P2Rs and IP_3Rs in hESCs and CVPCs. $n = 4–5$ independent experiments. $^{*}P < 0.05$, $^{**}P < 0.01$, $^{***}P < 0.001$ vs. the corresponding hESCs

Here, we detect the previously unrevealed contribution of P2R subtypes to Ca^{2+} responses in hESCs, though ATP, the nonselective agonist of P2Rs, has been found to be involved in the Ca^{2+} responses in mESCs [43] and hESCs [27]. In this study, we reveal that UTP and ADP but not UDP also trigger Ca^{2+} activities in hESCs. In contrast, all the nucleotides tested induce robust Ca^{2+} signals in the CVPCs. Moreover, distinct patterns of Ca^{2+} responses to these nucleotides are observed between the hESCs and CVPCs. The Ca^{2+} responses to ATP and UTP are more sensitive and stronger in the CVPCs than those in the hESCs, which may explain the recent finding that ATP treatment enhances cardiogenesis during mESC differentiation [23]. The differences could be interpreted by the distinct gene expression levels and selectivity of P2R subtypes in these cells (Fig. 4). Notably, only part of hESCs respond to UTP (Fig. 2b), a $P2Y_{2,4}$ receptor selective agonist [39]. Considering the correlation of cell surface proteins and pluripotency within hESCs [47], it is worthy to further investigate the physiological relevance of the UTP responding hESC subpopulation on the self-renewal and differentiation.

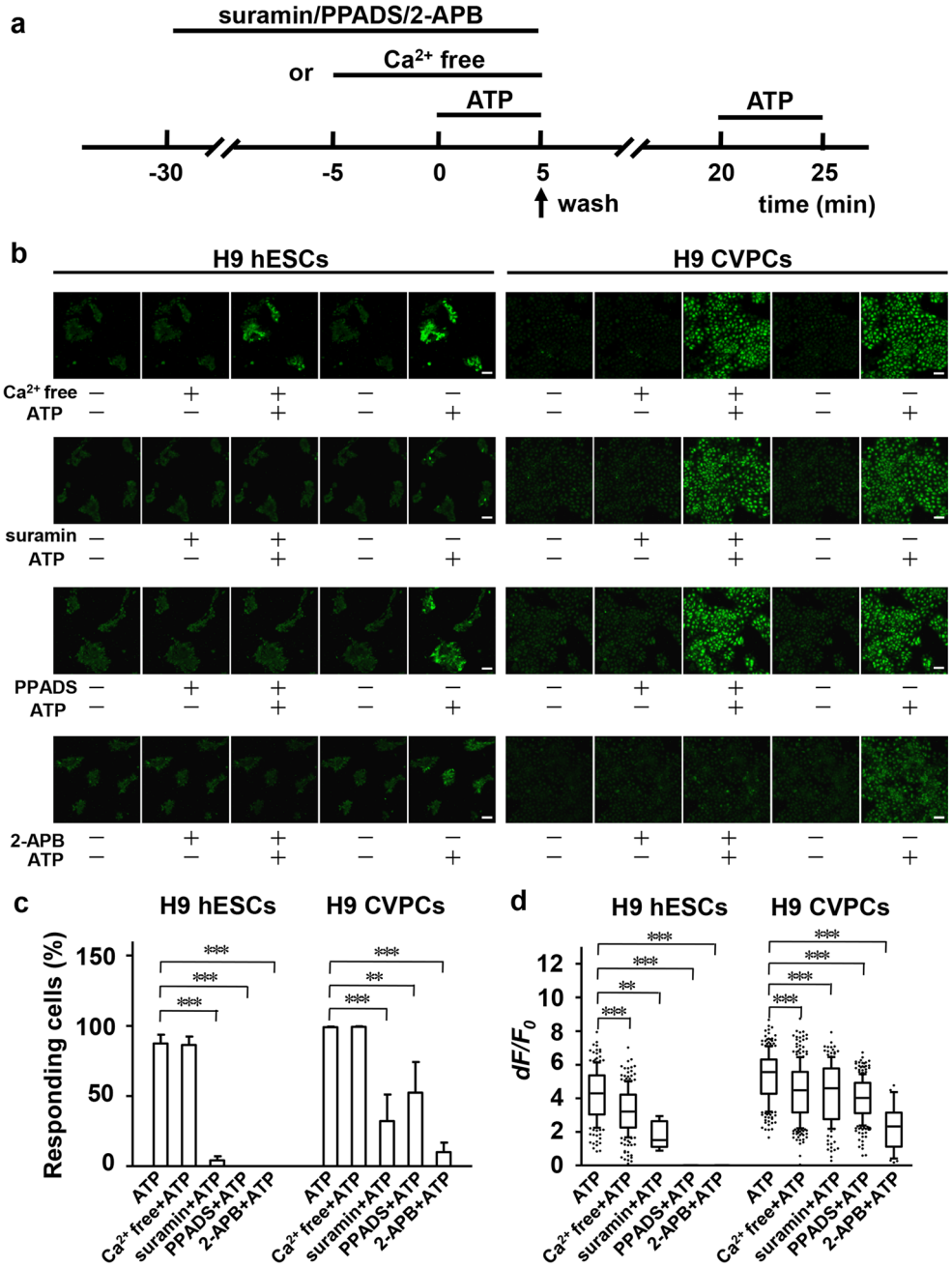

Fig. 5 Analysis of P2YRs and IP_3Rs involved in ATP-mediated Ca^{2+} events in H9 hESCs and CVPCs. **a** An outline of the experimental protocol. **b** Representative images showing the effects of extracellular Ca^{2+}-free solution, suramin, PPADS, and 2-APB on the Ca^{2+} responses induced by ATP in hESCs (*left*) and CVPCs (*right*). *Scale bar*, 50 μm. **c** The percentage of Ca^{2+} responding cells to ATP with or without various reagents. **d** Box whisker plots showing the median and 10–90 percentiles of the amplitudes (dF/F_0) of Ca^{2+} transients from responding cells to ATP with various pretreatments. *Dots* represent the outlier data of individual cells out of 10–90 percentiles. $n = 4–5$ independent experiments; 50–150 hESCs and 200–400 CVPCs in each experiment. $^{**}P < 0.01$, $^{***}P < 0.001$ vs. ATP alone

The Ca^{2+} signals mediated by the P2XR activation are observed in various cell types [48, 49]. The *P2rx3* and *P2rx4* genes are expressed in mESCs [24]. In our study, the gene expression of *P2RX2*, *P2RX5*, and *P2RX7* are detected in hESCs and *P2RX3* and *P2RX4* are detected in CVPCs (Fig. 4a). However, P2XRs seem to play a limited role in the Ca^{2+} responses of hESCs and CVPCs. This is supported by the following observations: (i) the responsive cell proportion remains unchanged in hESCs and CVPCs by removing extracellular Ca^{2+} which blocks the P2XR-mediated Ca^{2+} entry; (ii) almost no responses are detected in hESCs when triggered by the P2XR and $P2Y_1$ receptor nonselective agonist 2-MeSATP at the presence of $P2Y_1$ receptor selective antagonist MRS2279 (Fig. 6f) and few responses are triggered by 2-MeSATP in CVPCs (Fig. 6g); (iii) no responses are induced by the $P2X_7$ receptor agonist BzATP (data not shown) in hESCs and CVPCs. In contrast, the P2Y receptor agonists, such as ADP, UDP, UTP, and MRS2365, trigger distinct Ca^{2+} responses between hESCs and CVPCs, suggesting the important role of P2YR during the transition of hESCs to CVPCs (Fig. 3b). Taken together, our data here extend the previous findings by showing that the P2YRs but not P2XRs play crucial roles in nucleotide-mediated Ca^{2+} signals in hESCs and CVPCs. This is further confirmed by the inhibitory effect of 2-APB, an IP_3R

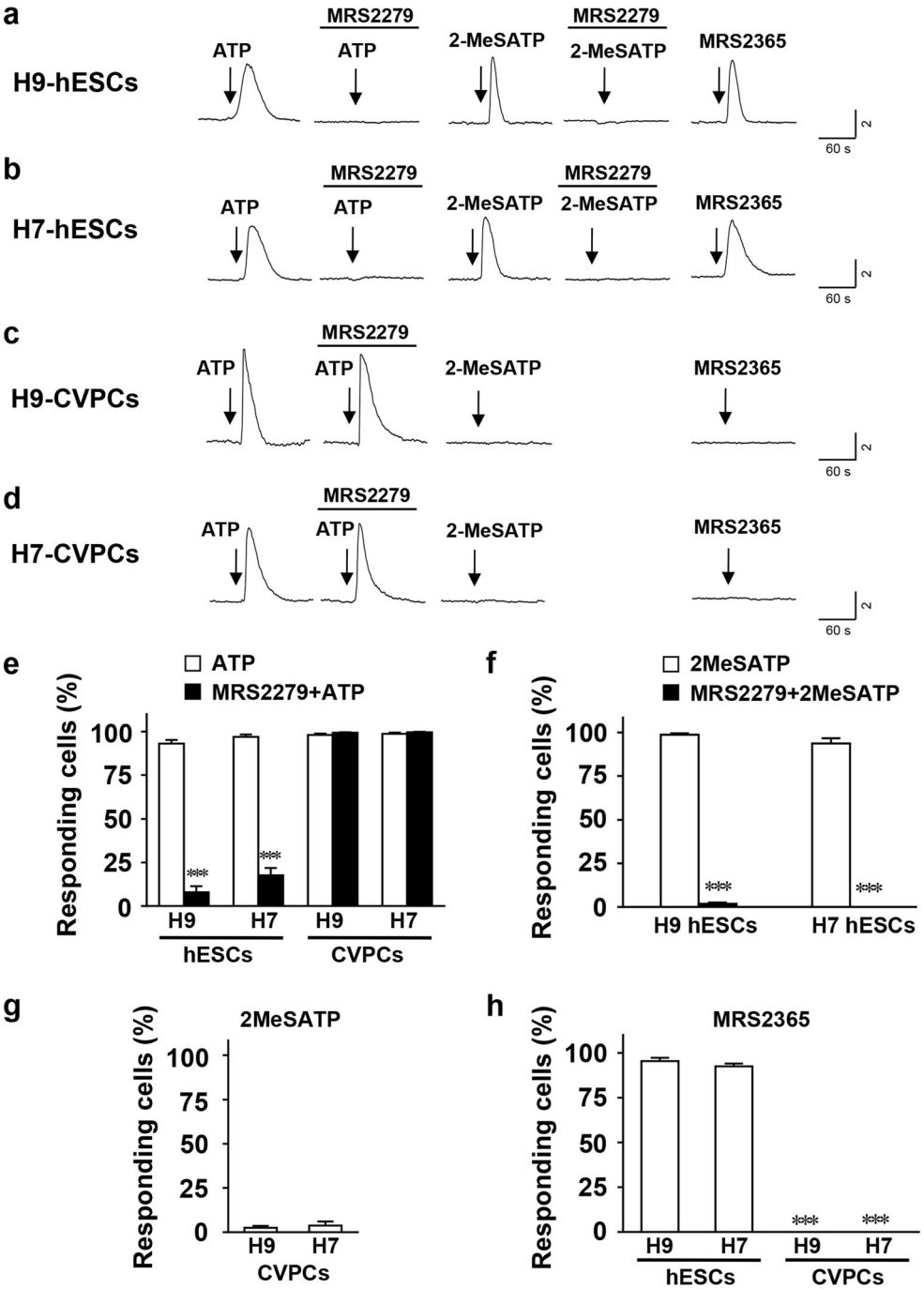

Fig. 6 $P2Y_1$ receptors primarily contributed to P2R-induced Ca^{2+} activity in hESCs not in CVPCs. **a**–**d** Representative traces of the Ca^{2+} transients from individual cells of hESCs (**a**, **b**) or CVPCs (**c**, **d**) treated with ATP (100 μM), 2-MeSATP (50 μM), or MRS2365 (50 μM) alone or combined with pre-incubation of MRS2279 (20 μM). **e** The cell percentages responding to ATP (100 μM) alone or pre-incubation with MRS2279 (20 μM) in hESCs and CVPCs. $n = 4–6$. $^{***}P < 0.001$ vs. ATP alone. **f** The cell percentages responding to 2-MeSATP (50 μM) alone or pre-incubation with MRS2279 (20 μM) in hESCs. $n = 4–5$. $^{***}P < 0.001$ vs. 2MeSATP alone. **g** The cell percentages responding to 2-MeSATP (100 μM) in CVPCs. $n = 4–5$. **h** The cell percentages responding to MRS2365 (50 μM) in hESCs and CVPCs. $n = 5$. $^{***}P < 0.001$ vs. the corresponding hESCs. *n*, number of independent experiments; 50–150 hESCs and 200–400 CVPCs in each experiment

antagonist [43], on the ATP-mediated Ca^{2+} signals in both cell types, suggesting the Ca^{2+} responses are mediated by P2YR-IP_3R coupling (Fig. 5c).

Notably, the contributions of P2YR subtypes are different between hESCs and CVPCs. Among most of the eight P2YR subtypes, $P2Y_1$ receptors predominantly mediate Ca^{2+} responses in the hESCs but not in the CVPCs. This is supported by the following evidence: firstly, $P2Y_1$ is the only P2YR subtype significantly reduced in the CVPCs compared with the hESCs (Fig. 4a, b); and secondly, the $P2Y_1$ receptor agonist MRS2365 [46] elicits Ca^{2+} transients in most hESCs. Meanwhile, the majority of the hESCs responding to ATP and 2MeSATP are blocked by MRS2279, a $P2Y_1$ receptor-specific antagonist [46]. Therefore, $P2Y_1$ receptors dominantly contribute to nucleotide-induced Ca^{2+} signals in the hESCs. Since the activation of $P2Y_1$ receptors in P19 embryonic carcinoma cells, a pluripotent stem cell line [50], has been reported to enhance the cell proliferation [51], it would be interesting to further determine the impact of this P2YR subtype in the regulation of proliferation of hESCs.

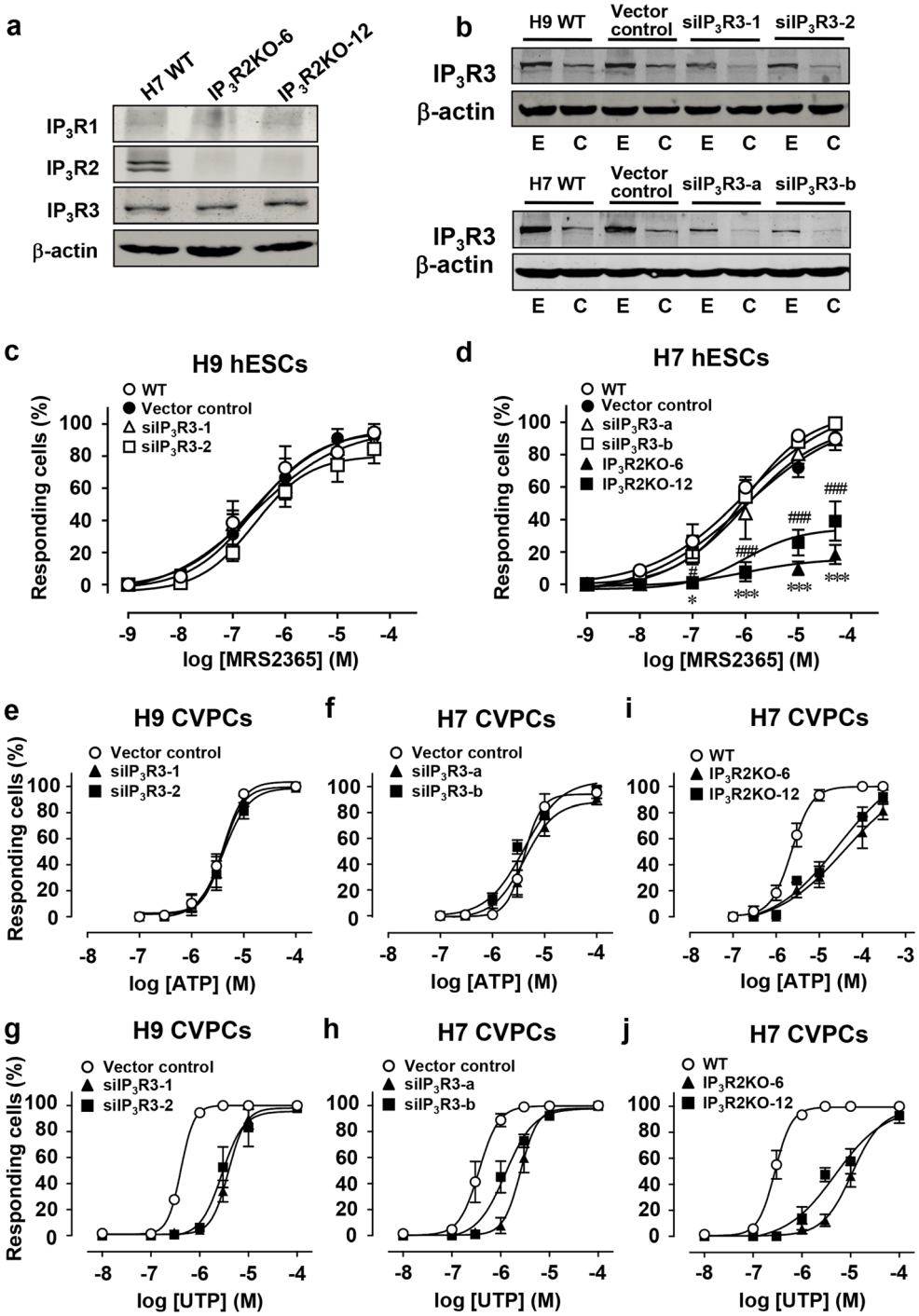

Fig. 7 Contributions of IP_3R2 and IP_3R3 to P2YR-mediated Ca^{2+} activity in hESCs and CVPCs. **a**, **b** The confirmation of IP_3R2KO (**a**) and IP_3R3KD (**b**) by Western blot analysis. *E*, hESCs; *C*, CVPCs. **c**, **d** Concentration-response curves of MRS2365 in the H9 (**c**) and H7 (**d**) IP_3R3KD hESCs or the IP_3R2KO hESCs (**d**). **e**–**h** The concentration-response curves of ATP (**e**, **f**) and UTP (**g**, **h**) in IP_3R3KD hESC-derived CVPCs. **i**, **j** The concentration-response curves of ATP (**i**) and UTP (**j**) in IP_3R2KO CVPCs. $n = 3$–4 independent experiments for each concentration; 50–150 hESCs and 200–400 CVPCs in each experiment. $^{*}P < 0.05$, $^{***}P < 0.001$ (IP_3R2KO-6) and $^{\#}P < 0.05$, $^{\#\#\#}P < 0.001$ (IP_3R2KO-12) vs. WT hESCs

All the genes encoding P2YRs are detectable in the CVPCs (Fig. 4a), while some of them may not functionally expressed like $P2Y_1$ and $P2Y_{11}$ (BzATP target [52]). Moreover, based on the different pharmacological profiles of P2YRs [28], the $P2Y_{2,4}$ receptor agonist UTP and the $P2Y_6$ receptor agonist UDP induce Ca^{2+} signals in almost 100 % CVPCs (Fig. 2a, b, Fig. 3c, d). Thus, the $P2Y_{2,4,6}$ receptors are significantly enhanced in the CVPCs compared with the hESCs, though other P2YR subtypes may also involve in the regulation of Ca^{2+} signals in CVPCs. These results indicate that the hESC-derived CVPCs are useful for the screening and pharmacological study of drugs targeting P2YRs.

Another finding here is the establishment of functional coupling of P2YRs and IP_3Rs in the regulation of intracellular Ca^{2+} release between the hESCs and CVPCs. The blockage of Ca^{2+} response by the IP_3R inhibitor 2-APB in hESCs and CVPCs suggests a crucial role of IP_3Rs in the purinergic signaling pathways of these cells. Since IP_3Rs are the

Table 1 EC_{50} values and slopes of ATP- and UTP-stimulated concentration-response curves in IP_3R3KD or IP_3R2KO CVPCs

Nucleotides	Cell lines	Gene manipulation	EC50 (μM)	Slopes	*n*
ATP	H9 CVPCs	Vector control	3.66	2.31	3
		siIP_3R3-1	4.14	2.18	3
		siIP_3R3-2	4.48	1.73	3
	H7 CVPCs	Vector control	4.25	2.46	3
		siIP_3R3-a	5.24	1.55	3
		siIP_3R3-b	2.75	1.46	3
	H7 CVPCs	WT	2.27	1.82	3
		IP_3R2KO-6	38.79	0.54	3
		IP_3R2KO-12	27.11	0.59	3
UTP	H9 CVPCs	Vector control	0.41	3.20	3
		siIP_3R3-1	3.90	2.46	4
		siIP_3R3-2	2.86	1.96	3
	H7 CVPCs	Vector control	0.36	2.13	5
		siIP_3R3-a	2.55	2.50	3
		siIP_3R3-b	1.25	1.48	3
	H7 CVPCs	WT	0.28	2.51	3
		IP_3R2KO-6	10.78	1.45	3
		IP_3R2KO-12	4.83	0.86	4

EC_{50} the effective concentration with 50 % maximal response, *Slopes* Hill slopes of nonlinear regression curves, *WT* wild type, *n* number of independent experiments for each concentration of the nucleotides

downstream of $P2Y_{1,2,4,6,11}$ receptor subtypes [15, 39] and the protein expression of IP_3R2 and IP_3R3 but not IP_3R1 are detected in hESCs in this study (Fig. 7a), it is conceivable to establish the coupling between $IP_3R2/3$ and P2YRs in the hESCs using gene manipulation. There are no changes of the $P2Y_1$ receptor agonist MRS2365-induced concentration-response curves in IP_3R3KD hESCs compared with the vector control and WT hESCs, while IP_3R2KO significantly decreases the responsive cell proportion to MRS2365 in hESCs, indicating a coupling of IP_3R2 to the $P2Y_1$ receptors in the hESCs. Thus, IP_3R2 but not IP_3R3 is essential for the Ca^{2+} signals mediated by the activation of $P2Y_1$ receptors in hESCs. Moreover, both IP_3R2 and IP_3R3 are involved in the regulation of Ca^{2+} responses in the CVPCs, while they differentially contribute to ATP- and UTP-induced Ca^{2+} activities (Fig. 7). The functional switch of IP_3Rs between hESCs and CVPCs may provide new clues for the dynamics of the intracellular Ca^{2+} mobilization in the early differentiating hESCs. Notably, although the gene expression of all IP_3R subtypes are lower in CVPCs than those in hESCs (Fig. 4a, c), the nucleotide-mediated Ca^{2+} transients are stronger (Fig. 2d, e). This may additionally due to the enhanced coupling between P2YRs and IP_3Rs or post-translational modifications on IP_3Rs [53]. The precise mechanisms underlying the heterogeneity of the Ca^{2+} responses and function of IP_3Rs in hESCs and CVPCs remain to be investigated.

Limitation: although our data are collected from two well-documented and wildly used cell lines, we cannot exclude the possibility that other hESCs and their derived CVPCs could display different P2Y and IP_3R expression patterns. Further

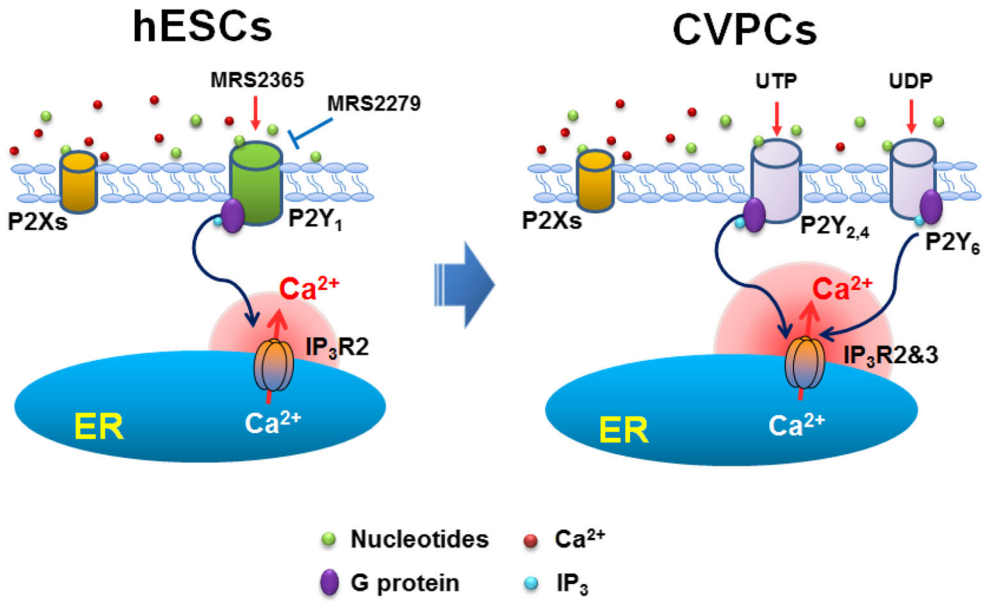

Fig. 8 A working model for the switch of functional coupling between P2YRs and IP_3Rs in hESCs and derived CVPCs. Ca^{2+} mobilization in hESCs and derived CVPCs is regulated by purinergic signals through the specific P2YR-IP_3R coupling, which results in the differential sensitivity and strength of Ca^{2+} responses between those cells. $P2Y_1$ receptors coupling to IP_3R2 are predominant in hESCs, while $P2Y_{2,4}$ receptors coupling to both IP_3R2 and IP_3R3 are enhanced in the CVPCs with a significantly decreased function of $P2Y_1$ receptors. In addition, $P2Y_6$ receptors are uniquely functional in the CVPCs but not in the hESCs. Little effect of P2XRs exists in the nucleotide-induced Ca^{2+} activities of hESCs and CVPCs

studies are needed to determine if the findings here can be extended to other hESC lines and their derived CVPCs.

Conclusion

Our results reveal that (i) a functional switch of P2YRs occurs between the hESCs and CVPCs; (ii) Ca^{2+} responses to various nucleotides are more sensitive and stronger in the CVPCs than those in the hESCs; (iii) $P2Y_1$ receptors coupling to IP_3R2 are the predominant P2YR subtype in hESCs, while $P2Y_{2,4}$ receptors coupled to $IP_3R2/3$ are enhanced in the CVPCs (Fig. 8). Our findings suggest that subtype-specific coupling and functional switch of P2YRs and IP_3Rs might play pivotal roles in the P2R-mediated Ca^{2+} signals in hESCs and CVPCs. The findings here would lead to a better understanding of the physiological and pharmacological properties of Ca^{2+} signal regulatory receptors in these cells.

Acknowledgments This work was supported by the grants from the National Natural Science of China Grants (Nos. 31030050 and 81520108004 to HTY, No. 31401167 to MZ); the Strategic Priority Research Program of CAS (No. XDA01020204 to HTY); the National Basic Research Program of China (No. 2014CB965100 to HTY); the National Science and Technology Major Project (No. 2012ZX09501001 to HTY); and the Major Program of Development Fund for Shanghai Zhangjiang National Innovation Demonstration Zone (No. ZJ2014-ZD-002 to HTY). We thank WiCell Research Institute for providing the H7 and H9 hESCs, and Dr. Heping Cheng (Peking University, Beijing, China) for providing the Flash Sniper software and for constructive discussion.

Compliance with ethical standards

Conflict of interest The authors declare that they have no conflicts of interest.

References

1. Yang L, Soonpaa MH, Adler ED, Roepke TK, Kattman SJ et al (2008) Human cardiovascular progenitor cells develop from a KDR^+ embryonic-stem-cell-derived population. Nature 453(7194):524–528
2. Birket MJ, Ribeiro MC, Verkerk AO, Ward D, Leitoguinho AR et al (2015) Expansion and patterning of cardiovascular progenitors derived from human pluripotent stem cells. Nat Biotechnol 33(9): 970–979
3. Bu L, Jiang X, Martin-Puig S, Caron L, Zhu S et al (2009) Human ISL1 heart progenitors generate diverse multipotent cardiovascular cell lineages. Nature 460(7251):113–117
4. Cao N, Liang H, Huang J, Wang J, Chen Y et al (2013) Highly efficient induction and long-term maintenance of multipotent cardiovascular progenitors from human pluripotent stem cells under defined conditions. Cell Res 23(9):1119–1132
5. Birket MJ, Mummery CL (2015) Pluripotent stem cell derived cardiovascular progenitors—a developmental perspective. Dev Biol 400(2):169–179
6. Pouton CW, Haynes JM (2007) Embryonic stem cells as a source of models for drug discovery. Nat Rev Drug Discov 6(8):605–616
7. Barbaric I, Gokhale PJ, Andrews PW (2010) High-content screening of small compounds on human embryonic stem cells. Biochem Soc Trans 38(4):1046–1050
8. Jung EM, Choi YU, Kang HS, Yang H, Hong EJ et al (2015) Evaluation of developmental toxicity using undifferentiated human embryonic stem cells. J Appl Toxicol 35(2):205–218
9. Jiang Y, Wang D, Zhang G, Wang G, Tong J et al (2015) Disruption of cardiogenesis in human embryonic stem cells exposed to trichloroethylene. Environ Toxicol. doi:10.1002/tox.22142
10. Blin G, Nury D, Stefanovic S, Neri T, Guillevic O et al (2010) A purified population of multipotent cardiovascular progenitors derived from primate pluripotent stem cells engrafts in postmyocardial infarcted nonhuman primates. J Clin Invest 120(4):1125–1139
11. Passier R, van Laake LW, Mummery CL (2008) Stem-cell-based therapy and lessons from the heart. Nature 453(7193):322–329
12. Kunapuli SP, Daniel JL (1998) P2 receptor subtypes in the cardiovascular system. Biochem J 336(Pt 3):513–523
13. Burnstock G, Pelleg A (2015) Cardiac purinergic signalling in health and disease. Purinergic Signalling 11(1):1–46
14. Erlinge D, Burnstock G (2008) P2 receptors in cardiovascular regulation and disease. Purinergic Signalling 4(1):1–20
15. Burnstock G (2014) Purinergic signalling: from discovery to current developments. Exp Physiol 99(1):16–34
16. Burnstock G, Ulrich H (2011) Purinergic signaling in embryonic and stem cell development. Cell Mol Life Sci 68(8):1369–1394
17. Li LF, Xiang C, Qin KR (2015) Modeling of TRPV4-C1-mediated calcium signaling in vascular endothelial cells induced by fluid shear stress and ATP. Biomech Model Mechanobiol 14(5):979–993
18. Nejime N, Tanaka N, Yoshihara R, Kagota S, Yoshikawa N et al (2008) Effect of P2 receptor on the intracellular calcium increase by cancer cells in human umbilical vein endothelial cells. Naunyn Schmiedeberg's Arch Pharmacol 377(4-6):429–436
19. Govindan S, Taylor CW (2012) P2Y receptor subtypes evoke different Ca^{2+} signals in cultured aortic smooth muscle cells. Purinergic Signalling 8(4):763–777
20. Kumari R, Goh G, Ng LL, Boarder MR (2003) ATP and UTP responses of cultured rat aortic smooth muscle cells revisited: dominance of P2Y2 receptors. Br J Pharmacol 140(7):1169–1176
21. Dolmatova E, Spagnol G, Boassa D, Baum JR, Keith K et al (2012) Cardiomyocyte ATP release through pannexin 1 aids in early fibroblast activation. Am J Physiol Heart Circ Physiol 303(10):H1208–1218
22. Cosentino S, Banfi C, Burbiel JC, Luo H, Tremoli E et al (2012) Cardiomyocyte death induced by ischaemic/hypoxic stress is differentially affected by distinct purinergic P2 receptors. J Cell Mol Med 16(5):1074–1084
23. Mazrouei S, Sharifpanah F, Bekhite MM, Figulla HR, Sauer H et al (2015) Cardiomyogenesis of embryonic stem cells upon purinergic receptor activation by ADP and ATP. Purinergic Signalling. 11(4): 491-506
24. Heo JS, Han HJ (2006) ATP stimulates mouse embryonic stem cell proliferation via protein kinase C, phosphatidylinositol 3-kinase/Akt, and mitogen-activated protein kinase signaling pathways. Stem Cells 24(12):2637–2648
25. Ferreira-Martins J, Rondon-Clavo C, Tugal D, Korn JA, Rizzi R et al (2009) Spontaneous calcium oscillations regulate human cardiac progenitor cell growth. Circ Res 105(8):764–774
26. Ermakov A, Pells S, Freile P, Ganeva VV, Wildenhain J et al (2012) A role for intracellular calcium downstream of G-protein signaling in undifferentiated human embryonic stem cell culture. Stem Cell Res 9(3):171–184

27. Apati A, Paszty K, Hegedus L, Kolacsek O, Orban TI et al (2013) Characterization of calcium signals in human embryonic stem cells and in their differentiated offspring by a stably integrated calcium indicator protein. Cell Signal 25(4):752–759
28. von Kugelgen I (2006) Pharmacological profiles of cloned mammalian P2Y-receptor subtypes. Pharmacol Ther 110(3):415–432
29. Mikoshiba K (2007) IP_3 receptor/Ca^{2+} channel: from discovery to new signaling concepts. J Neurochem 102(5):1426–1446
30. Foskett JK, White C, Cheung KH, Mak DO (2007) Inositol trisphosphate receptor Ca^{2+} release channels. Physiol Rev 87(2):593–658
31. Nakazawa M, Uchida K, Aramaki M, Kodo K, Yamagishi C et al (2011) Inositol 1,4,5-trisphosphate receptors are essential for the development of the second heart field. J Mol Cell Cardiol 51(1):58–66
32. Woodcock EA, Matkovich SJ (2005) Ins(1,4,5)P3 receptors and inositol phosphates in the heart-evolutionary artefacts or active signal transducers? Pharmacol Ther 107(2):240–251
33. Yoo SH (2012) Chromogranins and inositol 1,4,5-trisphosphate-dependent Ca(2+)-signaling in cardiomyopathy and heart failure. Curr Med Chem 19(24):4068–4073
34. Cao N, Liang H, Yang HT (2015) Generation, expansion, and differentiation of cardiovascular progenitor cells from human pluripotent stem cells. Methods Mol Biol 1212:113–125
35. He JQ, Ma Y, Lee Y, Thomson JA, Kamp TJ (2003) Human embryonic stem cells develop into multiple types of cardiac myocytes: action potential characterization. Circ Res 93(1):32–39
36. Li K, Zhang W, Liu J, Wang W, Xie W et al (2009) Flash Sniper: automated detection and analysis of mitochondrial superoxide flash. Biophys J 96(3):531a–532a
37. Hattori M, Suzuki AZ, Higo T, Miyauchi H, Michikawa T et al (2004) Distinct roles of inositol 1,4,5-trisphosphate receptor types 1 and 3 in Ca^{2+} signaling. J Biol Chem 279(12):11967–11975
38. Ouyang K, Leandro Gomez-Amaro R, Stachura DL, Tang H, Peng X et al (2014) Loss of IP3R-dependent Ca^{2+} signalling in thymocytes leads to aberrant development and acute lymphoblastic leukemia. Nat Commun 5:4814
39. Abbracchio MP, Burnstock G, Boeynaems JM, Barnard EA, Boyer JL et al (2006) International Union of Pharmacology LVIII: update on the P2Y G protein-coupled nucleotide receptors: from molecular mechanisms and pathophysiology to therapy. Pharmacol Rev 58(3):281–341
40. Zhang S, Fritz N, Ibarra C, Uhlen P (2011) Inositol 1,4,5-trisphosphate receptor subtype-specific regulation of calcium oscillations. Neurochem Res 36(7):1175–1185
41. James G, Butt AM (2002) P2Y and P2X purinoceptor mediated Ca^{2+} signalling in glial cell pathology in the central nervous system. Eur J Pharmacol 447(2-3):247–260
42. von Kugelgen I, Wetter A (2000) Molecular pharmacology of P2Y-receptors. Naunyn Schmiedeberg's Arch Pharmacol 362(4-5):310–323
43. Yanagida E, Shoji S, Hirayama Y, Yoshikawa F, Otsu K et al (2004) Functional expression of Ca^{2+} signaling pathways in mouse embryonic stem cells. Cell Calcium 36(2):135–146
44. Gur S, Hellstrom WJ (2009) Activation of P2Y1 and P2Y2 nucleotide receptors by adenosine 5′-triphosphate analogues augmented nerve-mediated relaxation of human corpus cavernosum. Can Urol Assoc J 3(4):314–318
45. Shen JB, Yang R, Pappano A, Liang BT (2014) Cardiac P2X purinergic receptors as a new pathway for increasing Na(+) entry in cardiac myocytes. Am J Physiol Heart Circ Physiol 307(10): H1469–1477
46. Govindan S, Taylor EJ, Taylor CW (2010) Ca(2+) signalling by P2Y receptors in cultured rat aortic smooth muscle cells. Br J Pharmacol 160(8):1953–1962
47. Hough SR, Laslett AL, Grimmond SB, Kolle G, Pera MF (2009) A continuum of cell states spans pluripotency and lineage commitment in human embryonic stem cells. PLoS One 4(11):e7708
48. Khaira SK, Pouton CW, Haynes JM (2009) P2X2, P2X4 and P2Y1 receptors elevate intracellular Ca^{2+} in mouse embryonic stem cell-derived GABAergic neurons. Br J Pharmacol 158(8):1922–1931
49. Mironneau J, Coussin F, Morel JL, Barbot C, Jeyakumar LH et al (2001) Calcium signalling through nucleotide receptor P2X1 in rat portal vein myocytes. J Physiol 536(Pt 2):339–350
50. Skerjanc IS (1999) Cardiac and skeletal muscle development in P19 embryonal carcinoma cells. Trends Cardiovasc Med 9(5):139–143
51. Resende RR, Britto LR, Ulrich H (2008) Pharmacological properties of purinergic receptors and their effects on proliferation and induction of neuronal differentiation of P19 embryonal carcinoma cells. Int J Dev Neurosci 26(7):763–777
52. Communi D, Robaye B, Boeynaems JM (1999) Pharmacological characterization of the human P2Y11 receptor. Br J Pharmacol 128(6):1199–1206
53. Bansaghi S, Golenar T, Madesh M, Csordas G, RamachandraRao S et al (2014) Isoform- and species-specific control of inositol 1,4,5-trisphosphate (IP_3) receptors by reactive oxygen species. J Biol Chem 289(12):8170–8181